Pure Appl. Chem., Vol. 85, No. 1, pp. 15–26, 2013.
http://dx.doi.org/10.1351/PAC-CON-12-04-08

Interactions between charged surfaces mediated by molecules with spatially distributed charges*

Klemen Bohinc

Faculty of Health Sciences, University of Ljubljana, Zdravstvena 5, SI-1000 Ljubljana, Slovenia

Abstract: A short review of recent theoretical advances in studies of the interaction between highly charged systems is presented. Such a system could not be described by the mean field theory. More advanced methods have to be used in order to introduce the correlations between highly charged particles. In this work I focus on the system of highly charged surfaces, separated by a solution of molecules with spatially distributed charge. Two different representations of the molecular shape will be considered: rod-like and spherical. The system will be theoretically described by the density functional theory. For sufficiently long molecules and large surface charge densities, an attractive force between like-charged surfaces arises due to the spatially distributed charges within the molecules. The added salt has influence on the condition for the attractive force between like-charged surfaces. The theoretical results will be compared with Monte Carlo (MC) simulations. Recent measurements with multivalent rigid rod-like particles will be discussed.

Keywords: biological interfaces; biomaterials; electrical double layer.

INTRODUCTION

In chemistry, technology, and biology, there are many phenomena which motivate the considerations of electrostatic interactions between charged macroions in a solution [1,2]. Usually the macroions appear as charged surfaces of mica, charged lipid membranes, DNA, colloids, actin molecules, proteins, viruses, and even cells. The intervening solution always contains simple salt and often also multivalent ions. The role of multivalent ions in the solution can be played by multivalent metal ions, charged micelles, dendrimers, polyelectrolytes including polyamines, and DNA. These ions mediate the electrostatic interaction between charged macroions. Generally, multivalent ions are needed to induce an attractive force between like-charged macroions. For example, divalent diamin ions induce the aggregation of rod-like M13 viruses [3]. Multivalent ions mediate network formation in actin solutions [4]. The condensation of DNA is induced by the presence of multivalent counterions [5,6]. Positively charged colloidal particles [7,8] complex with DNA. Even the cohesion of cement paste is controlled by divalent calcium counterions [9].

Many theories go beyond a simple Poisson–Boltzmann (PB) theory. The real ions are neither point-like nor can the solvent be regarded as passive and featureless. An extension of PB theory was made including ion correlations, charge images, and finite ion size. Many theories have been developed

Pure Appl. Chem.* **85, 1–305 (2013). A collection of invited papers based on presentations at the 32nd International Conference on Solution Chemistry (ICSC-32), La Grande Motte, France, 28 August–2 September 2011.

in order to include correlations: modified PB theory [10,11], liquid-state theories such as hypernetted-chain theories [12], loop expansions [13], variational approximations [14], and density functional theories [15,16]. In the limit of strong electrostatic coupling these theories break down and a strong coupling expansion theory can be introduced [17,18]. Recently, an approximative field theory has been developed that covers the weak, intermediate, and strong coupling regimes [19,20]. Image charge interactions were introduced as an additional external potential in PB theory [21], in integral equation theories [22,23], field theoretic methods [24], and variational approximation [25]. Dielectric heterogeneities were also studied in a strong electrostatic coupling [26]. The steric size of the ions has been accounted for by replacing the ideal gas with a lattice-gas [27–29], and also by using more involved density functional methods [30,31]. The possibility of specific adsorption of ions to charged surfaces was also considered. Stern [32] extended PB theory by dividing interfacial layer into adsorption and diffusive layers. A general method for including non-electrostatic interactions between ions into the PB formalism has been proposed [33].

The attractive force between like-charged macroions has been also confirmed by Monte Carlo (MC) simulations. Guldbrand et al. [34] first confirmed the existence of attraction between similarly charged surfaces immersed in a solution composed of divalent ions in the limit of high surface charge density. These and other MC simulations [35,37] demonstrated that attractive interactions between similarly charged surfaces may arise for sufficiently high surface charge densities, low temperatures, low relative permittivity, or polyvalent counterions. Recent MC simulations have provided that the existence of attractive interaction between like-charged surfaces is strongly conditioned by the finite size of ions [38].

Experimentally, the swelling of the lamellar liquid crystalline phase within the solution composed of monovalent or divalent ions [39] was studied. It was shown that replacing monovalent counterions with divalent ones drastically decreases swelling of lamellar phases [40]. The attractive interaction between bilayers in the presence of divalent calcium ions has been observed [41]. The short-range attractions between equally charged mica or clay surfaces in the solution of divalent ions have been detected in direct surface force measurements and atomic force microscopy [42].

The ions in a solution which mediate interactions between macroions usually have an internal structure, with individually separated charges and possibly with additional internal degrees of freedom. Recently, Bohinc et al. [43–46] demonstrated that intra-ionic correlations induced by the fixed distance within a particular rod-like ion are enough to change repulsive into attractive interactions between like-charged surfaces. In this study, the rod-like ions carry a single elementary charge on each end. The minimum of the free energy occurs when the counterions are oriented perpendicularly to the like-charged surfaces, thus connecting them. MC simulations confirmed the theoretical predictions [45–48]. The analysis of the system was later extended to the intermediate and strong coupling regimes, where the interionic correlations alone can lead to an attraction between the surfaces [49,50]. The theory was also generalized to systems with polydisperse rod lengths and arbitrary charge distribution along the rods. The influence of added salt was considered [51]. Also, the spherical ions were introduced in the system [52–54].

In this review article, I examine the interaction between two like-charged macromolecules which are represented by charged planar surfaces. The only interactions between the rod-like and spheroidal ions are the electrostatic interactions. We consider the conditions for attractive interactions mediated by rod-like or spheroidal ions. The influence of added salt is considered. We examine the appearance of attractive interactions between like-charged surfaces due to the internal structure of multivalent ions, as well as to the correlations between different ions.

THEORY

In order to examine the interaction between two macroions, we consider two parallel surfaces, separated by a distance D, which carry a uniform negative surface charge density σ. Between these surfaces is an aqueous solution containing charged, multivalent, rod-like, spherical, and point-like ions. Each rod-like or spherical ion carries two identical positive charges Ze, where e is the elementary charge and Z is the valency. The charges are separated by a fixed distance l. All charges are restricted to lie between the surfaces. A schematic diagram of the system is provided in Fig. 1. We define our Cartesian coordinate system such that the y-axis and z-axis are parallel to the surfaces, and the x-axis is perpendicular to both surfaces. The origin is located on the left surface.

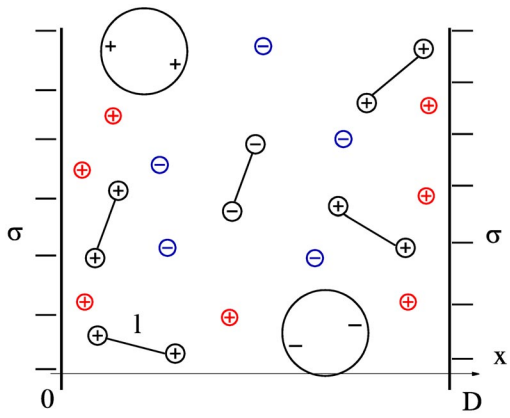

Fig. 1 Schematic presentation of two like-charged planar surfaces, located at $x = 0$ and $x = D$, with σ denoting the surface charge density. Each surface has a surface area A. The surfaces are immersed in an electrolyte solution that contains rod-like, spherical, and point-like ions. The rod-like and spherical ions have single elementary charge at each ending of the rod or sphere diameter.

The electrostatic field of the system varies only along the x-axis, the normal direction between the two charged surfaces. We assume that there is no electric field behind each of the two charged planar surfaces (which is appropriate if inside the macroions the dielectric constant is much smaller than in the aqueous region between the surfaces). Rod-like or spherical ions are characterized by positional and orientational degrees of freedom. We describe them by referring to one of the two charges of each ion as a reference charge, denoting the local concentration of all the reference charges by $n(x)$. The location of the second charge of a given ion is then specified by the conditional probability density $p(s \mid x)$, denoting the probability to find the second charge at position $x + s$ if the first resides at x. Thus the ion distribution function is defined as joint probability $n(x,s) = n(x)\, p(s \mid x)$. Integration over all possible orientations gives

$$n(x) = \frac{1}{2l} \int_{-l}^{l} n(x,s)\, \mathrm{d}s \tag{1}$$

The free energy F in terms of thermal energy $k_\mathrm{B}T$ and surface area A can be written as

$$\frac{F}{A\, k_\mathrm{B} T} = \frac{1}{8\pi l_\mathrm{B}} \int_{-\infty}^{\infty} \mathrm{d}x\, \Psi'(x)^2 + \int_{-\infty}^{\infty} \mathrm{d}x\, \frac{1}{2l} \int_{-l}^{l} \mathrm{d}s\, n(x,s) \left[\ln n(x,s) v - 1 - U(x,s) \right] \tag{2}$$

where v is the effective volume of counterions and Ψ is the reduced electrostatic potential. The prime in $\Psi'(x)$ denotes the first derivative with respect to the argument x. The Bjerrum length in water at a

room temperature is l_B = 0.714 nm. The first term in eq. 2 corresponds to mean electrostatic field energy, whereas the second term includes the orientational and positional entropic contribution of rod-like or spherical counterions. The steric interaction of rods or spheres with the charged surfaces is taken into account via the external non-electrostatic potential $U(x,s)$. The electro-neutrality of the whole system demands $\sigma = e\int_0^D n(x)\,\mathrm{d}x$.

In thermal equilibrium the free energy F adopts a minimum with respect to the ion distribution function. The functional minimization leads to the modified Boltzmann distribution function

$$n(x,s) = \frac{1}{v} e^{-\Psi(x)-\Psi(x+s)-U(x,s)} \tag{3}$$

Upon insertion of the ion distribution function (eq. 3) into Poisson's equation results in the integral differential equation

$$\Psi''(x) = -\frac{8\pi l_B}{v} \cdot \frac{1}{2l} \int_{\alpha(x)}^{\beta(x)} \mathrm{d}s\; e^{-\Psi(x)-\Psi(x+s)} \tag{4}$$

In the case of rod-like ions $\alpha(x)$ = max[$-l$,–x] and $\beta(x)$ = min[l,$D - x$] whereas in the case of spherical ions $\alpha(x)$ = max[$-l$,$l - 2x$] and $\beta(x)$ = min[l,$2D - 2x - l$].

If the solution is composed of rod-like or spherical counterions and monovalent salt (positive and negative point-like ions) the integral differential equation becomes

$$\Psi''(x) = -\frac{8\pi l_B}{v} \cdot \frac{1}{2l} \int_{\alpha(x)}^{\beta(x)} \mathrm{d}s\; e^{-\Psi(x)-\Psi(x+s)} - 4\pi l_B \sum_i i\, n_{si}\, e^{-i\Psi(x)} \tag{5}$$

Where n_{si} is a bulk concentration of the added salt, the sum runs over monovalent pointlike counterions (i = +) and coions (i = –).

The boundary conditions are given at both charged surfaces

$$\Psi'(0) = -4\pi l_B \frac{\sigma}{e} \tag{6}$$

and

$$\Psi'(D) = +4\pi l_B \frac{\sigma}{e} \tag{7}$$

They are equivalent to the overall electro-neutrality of the system.

RESULTS AND DISCUSSION

Integral differential equations (eqs. 4, 5) have no analytical solutions. The following analysis is based on the numerical solution of integral differential equations (eqs. 4 or 5).

First we examine the properties of divalent rod-like counterions confined between two like-charged surfaces separated by a distance D. Figure 2 shows the concentration of reference charges $n(x)$ as a function of the distance from the left-charged surface x for three different lengths l of rod-like ions [46]. The inset of Fig. 2 shows the reduced electrostatic potential $\Psi(x)$ as a function of the distance x from the charged surface. Theoretical results are compared against MC data. Figure 2, left, shows the results for counterions only, whereas the right side shows the results for counterions and coions. The concentration of reference charges decreases with increasing distance from the left charged surface to the value in the midplane of the system. The discontinuous derivative of concentration of reference charges $n(x)$ at $x = l$ and $x = D - l$ marks the orientational restriction of counterions close to the charged surface. For sufficiently long divalent rod-like counterions the comparison between the density func-

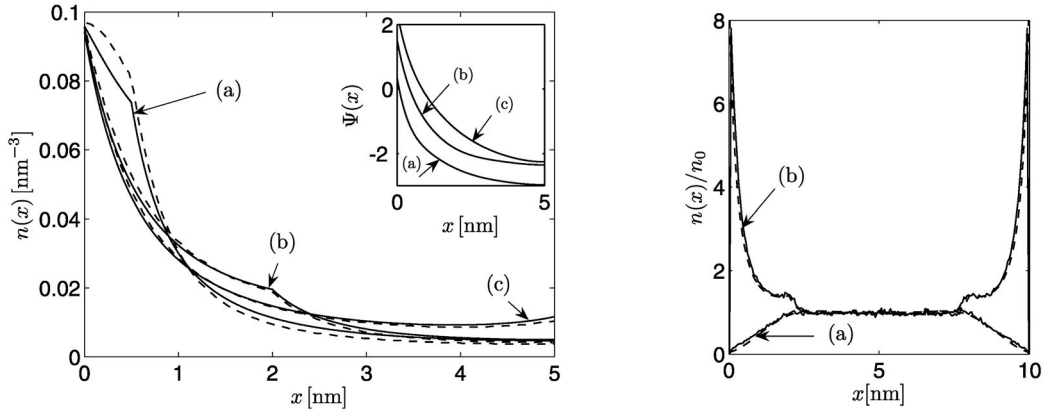

Fig. 2 Left: Concentration of reference charges $n(x)$ as a function of x. The different curves correspond to different lengths of divalent rod-like counterion $l = 0.5$ nm (a), $l = 2$ nm (b), and $l = 5$ nm (c). Full lines display the theoretical approach, whereas dashed lines display results of MC simulations. The inset shows reduced electrostatic potential $\Psi(x)$ as a function of x. The model parameters are $D = 10$ nm, $Z = 1$, and $\sigma = 0.033$ As/m^2. Right: Counterions (a) and coions (b) are present. Dashed lines display the theoretical approach, whereas full lines display results of MC simulation. The model parameters are: the length of the rod-like ions $l = 2$ nm, their bulk concentration $n_0 = 0.1$ mol/l and surface charge density $\sigma = 0.036$ As/m^2. Reprinted with permission from ref. [45,46].

tional theory and the MC simulations gives a good agreement. Also the non-continuous derivative of the concentration $n(x)$ at $x = l$ and $x = D - l$ is reproduced by MC simulations [46].

We proceed with the profiles for spherical ions. For distances between the surfaces, which are comparable to the diameter of spheres, the charge density profile in the solution shows a single peak at each side (Fig. 3). The spherical counterions, on the average, orient to form bridging between the charged surfaces [52]. For double diameter distances between the surfaces, we observe a peak in the middle which corresponds to "interdigitation" of the ordered counterions. Charges of spherical counterions of both layers contribute in the center of the system so a central peak in the charge density is

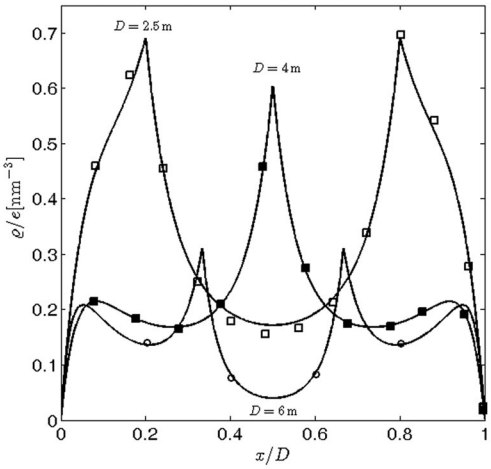

Fig. 3 Volume charge density of spherical counterions $\rho(x)$ as a function of x. The different curves correspond to different distances between the surfaces. The diameter of spheres is $l = 2$ nm. The lines display the theoretical approach whereas the signs display results of MC simulations. The model parameters are $Z = 1$ and $\sigma = 0.07$ As/m^2. Changed and reprinted with permission from ref. [52].

formed. For larger distances, we get two independent surfaces. The profile exhibits twin peaks close to both charged surfaces due to orientational ordering of spherical counterions with one charge closest to the charged surface. A very good agreement between the calculated density profile and the results of MC simulations is obtained [52].

Next we analyze the free energy and the pressure between like-charged planar surfaces. The osmotic pressure due to counterions between two like-charged surfaces can be calculated from the first derivative of the free energy with respect to plate separation $p = -\partial F/A\partial D$ [46]. Figure 4 shows the free energy as a function of the distance between two charged surfaces for two different lengths of rod-like ions. The energetically most favorable situation is at the pressure equal to zero. The analysis of the conditional probability density shows that the energetically most favorable distance between the charged surfaces corresponds to the length of the rod-like counterions. At this distance between the surfaces there are two most probable orientations of divalent rod-like counterions: counterions that are oriented parallel and perpendicular to the charged surfaces. Other orientations of rod-like counterions are less pronounced. The parallel and perpendicular orientations indicate the tendency of counterion charges to be in contact with the negatively charged surface. For high surface charge densities, both preferred orientations are even pronounced. The counterions that are oriented perpendicular to the charged surfaces connect both surfaces and act as a bridge between equally charged surfaces. This bridging mechanism of rod-like charged counterions is responsible for the attractive interaction between like-charged surfaces.

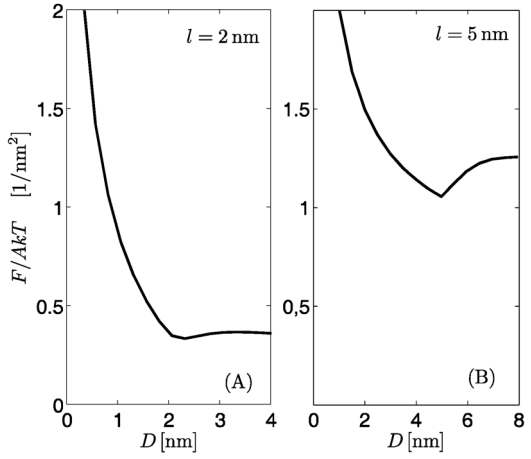

Fig. 4 Free energy F as a function of the distance between the charged surfaces D. The curves correspond to theoretical calculations. The model parameter is $\sigma = 0.1$ As/m^2. The length of ions is $l = 2$ nm (A) and $l = 5$ nm (B). Changed and reprinted with permission from ref. [46].

We proceed with the electrostatic free energy for a system where the salt of monovalent ion is included. The minimized expressions for the electrostatic potential and ionic distribution function are inserted back into the free energy. Figure 5 shows the equilibrium free energy as a function of the separation between the charged surfaces for three different salt concentrations. The free energy first decreases with increasing distance D, reaches a minimum and than further increases with increasing distance D to a plateau value. The minimum in the free energy appears at the distances that are approximately equal to the length of rod-like ions. The increasing salt concentration has very large impact on the minimum. For sufficiently large salt concentration the minimum in the free energy disappears [45]. The reason is the screening of charged surfaces by monovalent ions [51].

For small surface density of charge σ and small dimension of ions, the interaction is found to be repulsive for all distances between the charged surfaces. Large enough σ and l yield a non-monotonous

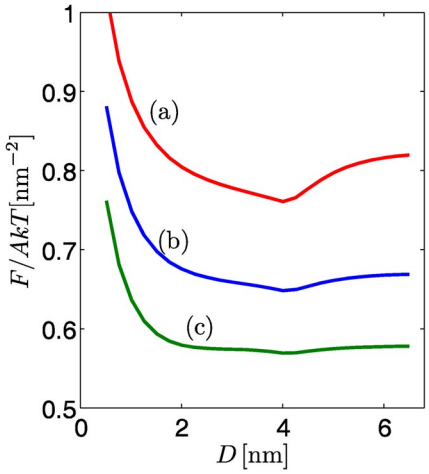

Fig. 5 Equilibrium electrostatic free energy as a function of the separation between charged surfaces. Three different curves corresponds to different salt concentrations (a) 0.001 mol/l, (b) 0.1 mol/l, and (c) 0.2 mol/l. The length of rod-like ions is $l = 4$ nm, and the surface charge density is $\sigma = 0.05$ As/m^2.

behavior of the free energy with a minimum representing the equilibrium distance between the surfaces [45].

In the limit of very low surface charge density, the mixtures of rod-like counterions and coions between two like surfaces exhibit quite different behavior. At larger separations between the surfaces, we observed that two flat surfaces no longer interact with each other (the free energy is for $D > l$ practically constant). For small distances, $l < D$, there is entropy loss of the mobile rods because of their interaction with both surfaces. The corresponding depletion attraction continues to dominate the system for weakly charged surfaces, leading to a minimum in free energy at very small separations between the surfaces [45]. For larger surface charge densities, the depletion minimum is absent. Generally we observe two minima in the free energy. The first minimum, located at small surface separations, corresponds to the depletion interaction and dominates at very low charged system. The second minimum, located roughly at $D \approx l$, dominates the system for larger surface charge densities. This second minimum is distinct from the depletion minimum; it is electrostatic in origin and can be ascribed to a bridging mechanism as analyzed below (see Fig. 6).

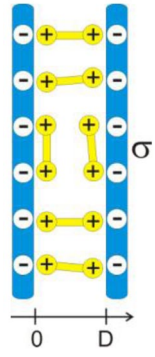

Fig. 6 Illustration of bridging between two charged surfaces induced by rod-like counterions. Reprinted with permission from ref. [6].

Figure 7 shows the conditional probability density as a function of the projection s of the rod-like counterions with respect to the x-axis [46]. Two different distances between the surfaces are considered. For large separation between the surfaces D, we observe an enhanced probability to find the second charge of the rod-like ion close to the macroion surface (see Fig. 7B). Clearly then, the rod-like ions exhibit a tendency to align parallel to the macroions' surface. For $D \approx l$ (see Fig. 7A), there are two regions of enhanced probability density, corresponding to the location of the rod-like ion's second charge close to either one of the macroion surfaces. Hence, our finding is that two different orientations are preferred, with the rod-like ion either parallel or normal to the macroions. It is the latter case that signifies the bridging transition.

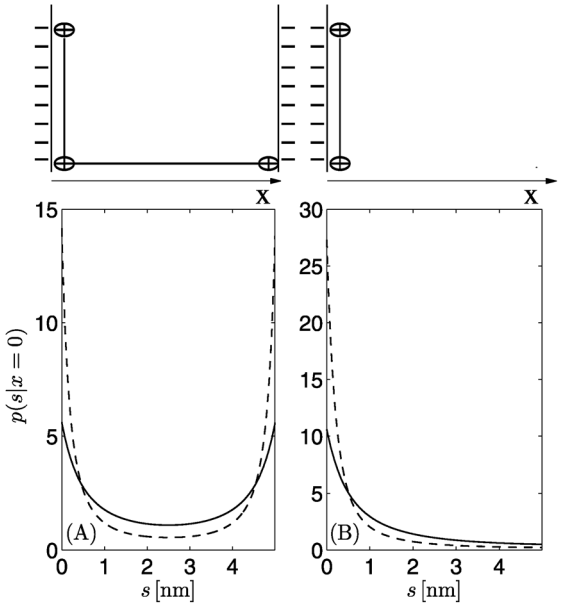

Fig. 7 Conditional probability densities $p(s \mid x = 0)$ as a function of the projection s of the rod-like counterions with respect to the x-axis. The distance between the charged surfaces is $D = 5$ nm (A) and $D = 20$ nm (B). The position $\sigma = 0.1$ As/m^2 of the reference charges was set to $x = 0$. The length of the rod was chosen to $l = 5$ nm. The full lines correspond to $\sigma = 0.033$ As/m^2, while the dashed lines correspond to $\sigma = 0.1$ As/m^2. The schematic presentation of the most probable orientations of rigid rod-like ions with the reference charges located at $x = 0$ (left charged surface) is shown on the top of the figure. In B, the right charged surface is not shown due to large distance D. Reprinted with permission from ref. [46].

The location of the bridging minimum in the free energy can be explained via analysis of the orientation of rod-like ions. At the distance between the surfaces equal to the length of rods, there are two most probable orientations of the rod-like ions: either oriented in parallel or perpendicular to the charged surfaces. Other orientations are less pronounced. The parallel and perpendicular orientations indicate the tendency for the positive part of rod-like ions to be in contact with the negatively charged surfaces. For high surface charge densities, both preferred orientations are even pronounced. The counterions that are oriented perpendicular to the charged surfaces connect both surfaces and act as a bridge between equally charged surfaces. This bridging mechanism of rod-like charged counterions is responsible for the attractive interaction between like-charged surfaces [52,62]. DNA packing in vivo is not only ion-dependent but is also governed by proteins. Proteins possess positively charged domains allowing nonspecific interactions with DNA. This type of interaction may be understood with the help

of a simplified model of two negatively charged surfaces (DNA molecules) in a solution of positively rod-like particles (proteins).

We adopted some simplifications in our model. First, we did not take into account the excluded volume of rod-like ions. In the systems that we consider, the Bjerrum length is much larger than the size of the counterions (e.g., spermidine molecules). Consequently, the electrostatic repulsion between the counterions does not allow them to get close enough for them to interact through excluded volume forces. This justifies the neglect of the excluded volume interactions. Second, the correlations between different rod-like ions were not taken into account. Third, we did not consider the partial adsorption of rod-like counterions on the charged surface. Fourth, we assumed uniformly distributed charge on the surfaces. In these studies, only electrostatic interactions are taken into account.

Charged interacting surfaces appear in different biological systems. Typical examples are charged colloidal particles, proteins, micelles, lamellar liquid crystals, and silica particles. These particles are significantly larger than mobile ions in the intervening solution. The intervening solution contains charge-neutralizing counterions and also coions of the same charge sign as the surfaces. Derjaguin–Landau–Verwey–Overbeek (DLVO) theory predicts stable colloidal systems even though the solution contains monovalent ions [55,56]. Replacing monovalent ions with divalent ones gives rise to attractive forces between colloidal particles, which was first observed for planar geometry [33,57] and then also for isotropic systems [58]. The presence of effective attraction between macroions is required for a system to undergo phase separation [59,60].

The presence of polycentric multivalent ions enhances the attraction between like-charged particles. Oppositely charged short polyions cause aggregation of colloidal particles by bridging mechanism [61], which was later confirmed by simulation studies [62,63] and supported by theoretical approaches [64]. Complex multivalent ions with spatially separated charge are also common in biological systems. Short polyamines spermine and spermidine, which play an important role in DNA packaging, are such examples [65,66,69].

Our study was motivated by a number of recent experiments, where the attractive interaction between equally charged macroions mediated by multivalent ions has been observed. The first observation of attraction between two highly negatively charged mica or clays was reported for the $CaCl_2$ solution [42,67]. Further examples are the network formation in actin solutions induced by divalent ions Ba^{2+} [4]. Attractive interactions between like-charged macroions can also arise through intra-ionic correlations, that is, correlations between the spatially separated charges of a single multivalent microion. A notable example is the ability of polyelectrolytes to complex oppositely charged macroions [68] as is observed for the condensation of DNA induced by cationic polymers [69]. The condensation of DNA can be induced by three- (four-) valent spermidines (spermines) [5,6]. The aggregation of viruses can be induced by divalent diamin ions [3]. Direct experimental observations of attractive, polyelectrolyte-induced forces, based on the surface force apparatus, have also been reported [70].

CONCLUSIONS AND OUTLOOK

In summary, we have developed a density functional theory for rod-like and spherical ions of arbitrary length, subject to an additional non-electrostatic external potential, which takes into account steric restrictions with the charged surface. The two interacting, like-charged, planar macroions reveal the possibility of attractive interactions, introduced entirely by correlations within the rod-like or spherical ions.

In the future, it would be also possible to study the influence of counterion valency and surface charge density for spherical ions on the interaction between like-charged surfaces. For rod-like ions, it was shown that the increased surface charge density is able to switch the bridging interaction into an attractive region at small surface separations [50]. This attraction is the result of charge correlations that become important for high surface charge densities and large ion valencies. These findings are the result of a self-consistent field theory, which treats the short- and long-range interactions of the counterions

within different approximations. In the intermediate coupling regime, the multivalent rod-like counterions can mediate attractive interactions between the surfaces. For sufficiently long rods, bridging contributes to the attractive interaction. In the strong coupling limit, the charge correlations can contribute to the attractive interactions at short separations between the charged surfaces (Fig. 8). Two minima can then appear in the force curve between surfaces.

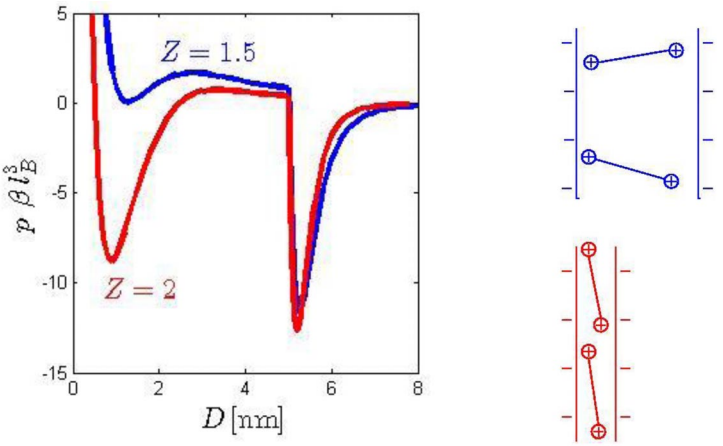

Fig. 8 Pressure as a function of the separation between the charged surfaces for rods of length $l = 5$ nm. The surface charge density is $\sigma = 0.1$ As/m^2. Reprinted with permission from ref. [50].

ACKNOWLEDGMENTS

The author acknowledges helpful discussions with Profs. S. May, L. Lue, J. M. A. Grime, V. Kralj-Iglič, J. Reščič, P. B. S. Kumar, and S. Maset.

REFERENCES

1. D. F. Evans, H. Wennerström. *The Colloidal Domain: Where Physics, Chemistry, Biology and Technology Meet*, Wiley-VCH, New York (1994).
2. S. McLaughlin. *Ann. Rev. Biophys. Biophys. Chem*. **18**, 113 (1989).
3. J. C. Butler, T. Angelini, J. X. Tang, G. C. L. Wong. *Phys. Rev. Lett.* **91**, 028301 (2003).
4. T. E. Angelini, H. Liang, W. Wriggers, G. C. L. Wong. *Proc. Natl. Acad. Sci. USA* **100**, 8634 (2003).
5. V. A. Bloomfield. *Curr. Opin. Struct. Biol.* **6**, 334 (1996).
6. V. B. Teif, K. Bohinc. *Prog. Biophys. Mol. Biol.* **105**, 208 (2011) .
7. J. O. Rädler, I. Koltover, T. Salditt, C. R. Safinya. *Science* **275**, 810 (1997).
8. W. M. Gelbart, R. Bruinsma, P. A. Pincus, V. A. Parsegian. *Phys. Today* **53**, 38 (2000).
9. B. Jönsson, A. Nonat, C. Labbez, B. Cabane, H. Wennerström. *Langmuir* **21**, 9211 (2005).
10. C. W. Outhwaite, L. B. Bhuiyan. *J. Chem. Soc., Faraday Trans. II* **79**, 707 (1983).
11. V. Vlachy. *Ann. Rev. Phys Chem.* **50**, 145 (1999).
12. M. Fushiki. *Chem. Phys. Lett.* **154**, 77 (1989).
13. R. D. Coalson, A. Duncan. *J. Chem. Phys*. **97**, 5653 (1992).
14. R. A. Curtis, L. Lue. *J. Chem. Phys*. **123**, 174702 (2005).
15. L. B. Bhuiyan, C. W. Outhwaite. *Condensed Matter Phys*. **8**, 287 (2005).
16. Y. X. Yu, J. Z. Wu, G. H. Gao. *Chin. J. Chem. Eng*. **12**, 688 (2004).
17. B. I. Shklovskii. *Phys. Rev. E* **60**, 5802 (1999).

18. A. G. Moreira, R. R. Netz. *Phys. Rev. Lett*. **87**, 078301 (2001).
19. M. M. Hatlo, A. Karatrantos. L. Lue. *Phys. Rev. E* **80**, 061107 (2009).
20. M. M. Hatlo, L. Lue. *Eur. Phys. Lett*. **89**, 25002 (2010).
21. C. Wagner. *Phys. Z.* **25**, 474 (1924).
22. R. Kjellander, S. Marcelja. *J. Chem. Phys*. **82**, 122 (1985).
23. P. Attard, D. J. Mitchell, B. W. Ninham. *J. Chem. Phys*. **88**, 4987 (1988).
24. R. R. Netz. *Eur. Phys. J. E* **5**, 557 (2001).
25. M. Hatlo, L. Lue. *Soft Matter* **4**, 1 (2008).
26. Y. S. Jho, M. Kanduč, A. Naji, R. Podgornik, M. W. Kim, P. A. Pincus. *Phys. Rev. Lett*. **101**, 188101 (2008).
27. J. R. Macdonald. *J. Electroanal. Chem*. **223**, 1 (1987).
28. V. Freise. *Z. Elektrochem*. **56**, 822 (1952).
29. S. Lamperski, C. W. Outhwaite. *Langmuir* **18**, 3423 (2002).
30. D. Antypov, M. C. Barbosa, C. Holm. *Phys. Rev. E* **71**, 061106 (2005).
31. L. B. Bhuiyan, C. W. Outhwaite. *J. Colloid Interface Sci*. **331**, 543 (2009).
32. O. Stern. *Z. Elektrochem*. **30**, 508 (1924).
33. L. Lue, N. Zoeller, D. Blankschtein. *Langmuir* **15**, 3726 (1999).
34. L. Guldbrand, B. Jönsson, H. Wennerström, P. Linse. *J. Chem. Phys*. **80**, 2221 (1984).
35. B. Svensson, B. Jönsson. *Chem. Phys. Lett*. **108**, 580 (1984).
36. A. G. Moreira, R. R. Netz. *Phys. Rev. Lett.* **87**, 078301 (2001).
37. J. Reščič, P. Linse. *J. Phys. Chem. B* **104**, 7852 (2000).
38. A. Martín-Molina, J. G. Ibarra-Armenta, E. González-Tovar, R. Hidalgo-Álvarez, M. Quesada-Pérez. *Soft Matter* **7**, 1441 (2011).
39. A. Khan, K. Fontell, B. Lindman. *J. Colloid Interface Sci*. **101**, 193 (1984).
40. H. Wennerström, A. Khan, B. Lindman. *Adv. Colloid Interface Sci*. **34**, 433 (1991).
41. J. Marra. *Biophys. J*. **50**, 815 (1986).
42. R. Kjellander, S. Marčelja, R. M. Pashley, J. P. Quirk. *J. Phys. Chem*. **92**, 6489 (1988).
43. K. Bohinc, A. Iglič, S. May. *Europhys. Lett*. **68**, 494 (2004).
44. S. Maset, K. Bohinc. *J. Phys. A: Math. Theor.* **40**, 1 (2007).
45. S. May, A. Iglič, J. Reščič, S. Maset, K. Bohinc. *J. Phys. Chem. B* **112**, 1685 (2008).
46. S. Maset, J. Reščič, S. May, J. I. Pavlič, K. Bohinc. *J. Phys. A* **42**, 105401 (2009).
47. Y. W. Kim, J. Yi, P. A. Pincus. *Phys. Rev. Lett*. **101**, 208305 (2008).
48. M. A. Grime, M. O. Khan, K. Bohinc. *Langmuir* **26**, 6343 (2010).
49. M. M. Hatlo, K. Bohinc, L. Lue. *J. Chem. Phys*. **132**, 114102 (2010).
50. K. Bohinc, L. Lue. *Chin. J. Polym. Sci*. **29**, 414 (2011).
51. K. Bohinc, J. Reščič, S. Maset, S. May. *J. Phys. Chem.* **134**, 074111 (2011).
52. J. Urbanija, K. Bohinc, A. Bellen, S. Maset, A. Iglič, V. Kralj-Iglič, P. B. S. Kumar. *J. Chem. Phys.* **129**, 105101 (2008).
53. Š. Perutkova, M. Frank, K. Bohinc, G. Bobojevič, J. Zelko, B. Rozman, V. Kralj-Iglič, A. Iglič. *J. Membr. Biol.* **236**, 43 (2010).
54. S. May, K. Bohinc. *Croat. Chem. Acta* **84**, 251 (2011).
55. B. V. Derjaguin, L. D. Landau. *Acta Physicochim. URSS* **14**, 633 (1941).
56. E. J. Vervey, J. T. G. Overbeek. *Theory of the Stability of Lyophobic Colloids*, Elsevier, Amsterdam (1948).
57. J. P. Valleau, R. Ivkov, G. M. Torrie. *J. Chem. Phys*. **95**, 520 (1991).
58. B. Hribar, V. Vlachy. *J. Phys. Chem. B* **101**, 3457 (1997).
59. V. Lobaskin, P. Linse. *Phys. Rev. Lett.* **83**, 4208 (1999).
60. J. Reščič, P. Linse. *J. Chem. Phys.* **114**, 10131 (2001).
61. R. J. Hunter. *Foundations of Colloid Science*, Vol. 1, Oxford Science Publications (1987).
62. M. Jönsson, P. Linse. *J. Chem. Phys*. **115**, 3406 (2001).

63. J. Reščič, P. Linse. *J. Phys. Chem. B* **104**, 7852 (2000).
64. R. Podgornik. *J. Polym. Sci., Part B: Polym. Phys.* **42**, 3539 (2004).
65. V. A. Bloomfield. *Curr. Opin. Struct. Biol*. **6**, 334 (1996).
66. B. Jönsson, H. Wennerström, B. Halle. *J. Phys. Chem.* **84**, 2179 (1980).
67. R. Kjellander, S. Marcelja, R. M. Pashley, J. P. Quirk. *J. Chem. Phys*. **92**, 4399 (1990).
68. J. Forsman. *Curr. Opin. Colloid Interface Sci*. **11**, 290 (2006).
69. X. Liu, J. W. Yang, A. D. Miller, A. E. Nack, D. M. Lynn. *Macromolecules* **38**, 7907 (2005).
70. P. M. Claesson, E. Poptoshev, E. Blomberg, A. Dedinaite. *Adv. Colloid Interface Sci*. **114–115**, 173 (2005).

